Electronic Supplementary Material (ESI) for Physical Chemistry Chemical Physics.

Hole-Transport Materials with Greatly-differing Redox Potentials give Efficient TiO_2-[CH_3NH_3]PbI_3] Perovskite Solar Cells.

Antonio Abate,[b] Miquel Planells,[a] Vishal Barthi,[c] Suresh Chand,[c] Henry J. Snaith[b]* and Neil Robertson[a]*

Supplementary Information

TABLE OF CONTENTES

Experimental procedure

The synthesis of **Me_2N-DATPA** was attained in a similar fashion to **MeO-DATPA** which we have previously reported[1] and it is shown in Scheme 1. All materials were commercially available and used without further purification unless otherwise stated.

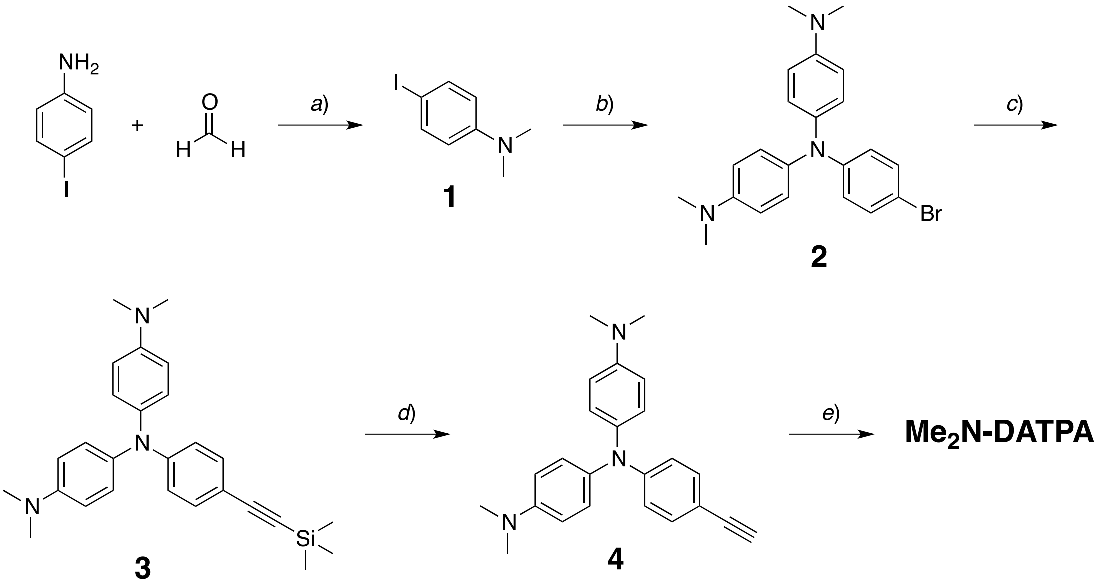

Scheme S1. Synthetic procedure for **Me_2N-DATPA**. Reaction conditions: (*a*) $NaBH_4$, H_2SO_4, THF; (*b*) 4-bromoaniline, CuI, bipy, KOtBu, toluene; (*c*) triethylsilylacetylene, $(PPh_3)_2PdCl_2$, PPh_3, CuI, piperidine, toluene; (*d*) 1 M TBAF, CH_2Cl_2; (*e*) CuCl, TMEDA, O_2, CH_2Cl_2.

Synthesis of 4-iodo-*N*,*N*-dimethylaniline (1). A previously made solution of 4-iodoaniline (25 g, 114 mmol) and finely grounded $NaBH_4$ (25.9 g, 684 mmol) in 230 mL of THF was added drop-wise to 350 mL of 0.5 M aqueous H_2SO_4 with 37 % aqueous formaldehyde (37g, 0.456 mmol) at 0 ºC. After addition, the pH was adjusted to 13 by using aqueous NaOH. The crude was extracted in Et_2O (x2), washed with water and brine. Organic layers were collected, dried over Na_2SO_4 and the solvent removed. Pure product was afforded by silica plug in $CHCl_3$ as pale grey solid (19.5 g, 69% yield). ^1H NMR (500 MHz, $CDCl_3$) δ_H: 7.47 (d, J = 9.0 Hz, 2H); 6.50 (d, J = 9.0 Hz, 2H); 2.93 (s, 6H). ^{13}C NMR (125 MHz, $CDCl_3$) δ_C: 150.1; 137.7; 114.9; 77.7; 40.6. MS EI (m/z): $[M]^+$ calcd for $C_8H_{10}IN$: 246.98524; found: 246.985051. Anal. Calcd for $C_{22}H_{24}BrN_3$: C, 38.89; H, 4.08; N, 5.67; Found: C, 38.93; H, 4.14; N, 5.71.

Synthesis of *N*^{1}-(4-bromophenyl)-*N*^{1}-(4-(dimethylamino)phenyl)-*N*^{4},*N*^{4}-dimethylbenzene-1,4-diamine (2). **1** (8.22 g, 33.3 mmol), 4-bromoaniline (1.92 g, 11.1 mmol), potassium *tert*-butoxide (5 g, 44.4 mmol), copper iodide (85 mg, 0.444 mmol) and 2,2'-bipyridyl (69 mg, 0.444 mmol) were placed in a round bottom flask and dried under high vacuum for 30 minutes. Previously degassed dry toluene (45 mL) was added and the mixture was stirred at 120 ºC overnight under N_2. Then, a silica plug was run in CH_2Cl_2 and the solvent removed. The crude product was further purified by column chromatography (SiO_2, Hexanes / EtOAc 10:1) to afford the product as pale grey solid (1.08 g, 23% yield). ^{1}H NMR (500 MHz, DMSO-*d*$_6$) δ_H: 7.23 (d, *J* = 9.1 Hz, 2H); 6.95 (d, *J* = 8.8 Hz, 4H); 6.70 (d, *J* = 8.9 Hz, 4H); 6.58 (d, *J* = 8.9 Hz, 2H); 2.88 (s, 12H). ^{13}C NMR (125 MHz, DMSO-*d*$_6$) δ_C: 148.5; 147.6; 135.8; 131.3; 126.9; 118.9; 113.5; 109.1; 40.3. MS EI (m/z): $[M]^+$ calcd for $C_{22}H_{24}BrN_3$: 409.11481; found: 409.114607. Anal. Calcd for $C_{22}H_{24}BrN_3$: C, 64.39; H, 5.90; N, 10.24; Found: C, 64.29; H, 5.78; N, 10.12.

Synthesis of *N*^{1}-(4-(dimethylamino)phenyl)-*N*^{4},*N*^{4}-dimethyl-*N*^{1}-(4-((trimethylsilyl)ethynyl)phenyl)benzene-1,4-diamine (3). Bis(triphenylphosphine)palladium dichloride (74 mg, 0.105 mmol), triphenylphosphine (55 mg, 0.210 mmol) and copper iodide (60 mg, 0.315 mmol) were placed in a shlenck tube and dried under high vacuum for 30 minutes. Then, a previously degassed solution of **2** (1.08 g, 2.63 mmol), piperidine (2.1 mL, 21 mmol) and ethynyltrimethylsilane (1.45 mL, 7.89 mmol) in 21 mL of dry toluene was added *via* cannula. The mixture was degassed again by the pump/freeze technique and stirred at 80 ºC over 2 days under N_2. Then, a silica plug was run in CH_2Cl_2 and the solvent removed. The crude product was further purified by column chromatography (SiO_2, Hexanes / EtOAc 10:1) to afford the product as yellow solid (1.06 g, 94% yield). ^{1}H NMR (500 MHz, DMSO-*d*$_6$) δ_H: 7.15 (d, *J* = 9.0 Hz, 2H); 6.99 (d, *J* = 9.0 Hz, 4H); 6.71 (d, *J* = 9.0 Hz, 4H); 6.54 (d, *J* = 9.0 Hz, 2H); 2.87 (s, 12H); 0.18 (s, 9H). ^{13}C NMR (125 MHz, DMSO-*d*$_6$) δ_C: 149.5; 147.9; 135.1; 132.4; 127.4; 115.7; 113.4; 110.4; 106.5; 91.3; 40.3; 0.1. MS EI (m/z): $[M]^+$ calcd for $C_{27}H_{33}N_3Si$: 427.24383; found: 427.243305. Anal. Calcd for $C_{27}H_{33}N_3Si$: C, 75.83; H, 7.78; N, 9.83; Found: C, 75.67; H, 7.69; N, 9.76.

Synthesis of *N*^{1}-(4-(dimethylamino)phenyl)-*N*^{1}-(4-ethynylphenyl)-*N*^{4},*N*^{4}-dimethylbenzene-1,4-diamine (4). **3** (1.06 g, 2.48 mmol) was placed in a round bottom flask with 12.5 mL of CH_2Cl_2. Then, tetrabutylammonium fluoride 1 M in THF (3.72 mL, 3.72 mmol) was added and the mixture was stirred for 2 hours at room temp. under N_2. Then, a silica plug was run in CH_2Cl_2 and the solvent removed. The crude product was further purified by column chromatography (SiO_2, Hexanes / EtOAc 10:1) to afford the product as yellow solid (580 mg, 66% yield). ^{1}H NMR (500 MHz, DMSO-*d*$_6$) δ_H: 7.19 (d, *J* = 8.8 Hz, 2H); 6.99 (d, *J* = 8.8 Hz, 4H); 6.72 (d, *J* = 9.0 Hz, 4H); 6.57 (d, *J* = 8.8 Hz, 2H);

3.89 (s, 1H); 2.87 (s, 12H). ^{13}C NMR (125 MHz, DMSO-d_6) δ_C: 149.5; 147.9; 135.3; 132.4; 127.3; 116.0; 113.5; 110.1; 85.4; 78.3; 40.3. MS EI (m/z): $[M]^+$ calcd for $C_{24}H_{25}N_3$: 355.20430; found: 355.204490. Anal. Calcd for $C_{24}H_{25}N_3$: C, 81.09; H, 7.09; N, 11.82; Found: C, 78.37; H, 6.98; N, 11.19. Note that compound **4** was found to be unstable over time as evidenced by a colour change over one day. The need to send the sample externally for elemental analysis will have resulted in some decomposition hence the poor agreement of the numbers quoted above despite a clean NMR spectrum. Samples of **4** used for the synthesis of **Me$_2$N-DATPA** were used as soon as possible after synthesis.

Synthesis of *N*^{1},*N*$^{1'}$-(buta-1,3-diyne-1,4-diylbis(4,1-phenylene))bis(*N*^{1}-(4-(dimethylamino)phenyl)-*N*^{4},*N*^{4}-dimethylbenzene-1,4-diamine) (Me$_2$N-DATPA). **4** (355 mg, 1 mmol) was placed in a round bottom flask with 40 mL of CH_2Cl_2. TMEDA (1.65 mL, 1 mmol) and copper(I) chloride (990 mg, 10 mmol) were added and the mixture was stirred vigorously for 1.5 hours under air with a $CaCl_2$ tube on top. Then, a silica plug was run in CH_2Cl_2/EtOAc (10:1) and the solvent removed. The crude product was further purified by column chromatography (SiO_2, $CHCl_3$ / EtOAc 4%) to afford the product as yellow solid (267 mg, 75% yield). ^{1}H NMR (500 MHz, DMSO-d_6) δ_H: 7.26 (d, $J = 8.9$; 2H); 7.01 (d, $J = 8.9$, 4H); 6.73 (d, $J = 8.9$; 4H); 6.56 (d, $J = 8.9$, 2H); 2.88 (s, 12H). ^{13}C NMR (125 MHz, DMSO-d_6) δ_C: 150.0; 148.1; 134.8; 133.2; 127.5; 115.7; 113.4; 108.6; 82.7; 72.7; 40.3. MS EI (m/z): $[M]^+$ calcd for $C_{48}H_{48}N_6$: 708.39350; found: 708.392298. Anal. Calcd for $C_{48}H_{48}N_6$: C, 81.32; H, 6.82; N, 11.85; Found: C, 81.22; H, 7.00; N, 11.78.

Characterisation Methods

Chemical characterisation. ^{1}H and ^{13}C NMR spectra were recorded on Bruker Advance 500 spectrometer (500 MHz for ^{1}H and 125 MHz for ^{13}C). The deuterated solvents are indicated; chemical shifts, δ, are given in ppm, referenced to the solvent residual signal (^{1}H, ^{13}C). MS were recorded on ThermoElectron MAT 900 using electron impact (EI) ionization technique. Elemental analyses were carried out by Stephen Boyer at London Metropolitan University using a Carlo Erba CE1108 Elemental Analyser.

Electrochemical characterisation. All cyclic voltammetry measurements were carried out in freshly distilled CH_2Cl_2 using 0.3 M [TBA][PF_6] electrolyte in a three electrode system, with each solution being purged with N_2 prior to measurement. The working electrode was a Pt disk. The reference electrode was Ag/AgCl and the counter electrode was a Pt rod. All measurements were made at r.t. using an μAUTOLAB Type III potentiostat, driven by the electrochemical software GPES. Cyclic voltammetry (CV) measurements used scan rates of 25, 50, 100, 200 and 500 mV/s, and square wave voltammetry (SWV) was carried out at a step potential of 4 mV, a square wave amplitude of 25 mV and a square wave frequency of 15 Hz, giving a scan rate of 40 mV/s. Ferrocene was used as internal standard in each measurement.

Optical characterisation. Solution UV-Visible absorption spectra were recorded using Jasco V-670 UV/Vis/NIR spectrophotometer controlled using the SpectraManager software. Photoluminescence (PL) spectra were recorded with Fluoromax-3 fluorimeter controlled by the ISAMain software. All samples were measured in a 1 cm cell at r.t. with dichloromethane as a solvent. Concentration of $2 \cdot 10^{-5}$ M and $5 \cdot 10^{-6}$ M were used for UV/Vis and PL, respectively.

Computational details: The molecular structures were optimized first in vacuum without any symmetry constrains, followed by the addition of CH_2Cl_2 solvation via a conductor-like polarizable continuum model (C-PCM).[2] The presence of local minimum was confirmed by the absence of imaginary frequencies. All calculations were carried out using the Gaussian 09 program[3] with the Becke three parameter hybrid exchange, Lee Yang–Parr correlation functional (B3LYP) level of theory. All atoms were described by the 6-31G(d) basis set. All structures were input and processed through the Avogadro software package.[4]

Crystallographic details: Crystallographic data were collected on an Agilent Technologies SuperNova with Cu *K*α (λ = 1.54178 Å) radiation at 120 K. Single crystals suitable for X-ray diffraction (XRD) were prepared by layer addition of EtOAc into a concentrated DMSO solution. A summary of data collection and structure refinement is reported in Table S1. Programs used were: data collection and reduction, CrysAlisPro;[5] structure solution, Sir92;[6] structure refinement, SHELXTL.[7] The crystal structure was deposited at CCDC with deposition number 936124.

Charge transport parameters: Poly(3,4-ethylendioxythiophene)–poly(styrene sulfonate) (PEDOT:PSS) was spin-coated onto indium tin oxide substrate (ITO) and dried at 140 ºC for 30 min in vacuum. The purpose of PEDOT:PSS layer (40 nm) was to reduce the roughness of ITO as well as to improve the work function, achieving enhanced hole-only device properties. The HTMs were spin-coated onto PEDOT:PSS from chloroform solution (40 mg/mL) in a nitrogen atmosphere. Finally, Au contacts (400 nm thick) were applied via thermal evaporation through a shadow mask in 2×10^{-6} Torr vacuum. The work function of Au and ITO are close to the HOMO energy level of the HTM as well as far below the LUMO energy level. Therefore, the electron injection barrier is higher than the corresponding hole injection barrier. As a result, the transport is dominated by holes. The *J–V* characteristics of the sample was measured with a Keithley 2420 Source Meter unit at room temperature. The device configuration and equations to extract mobility has been reported by us previously.[1]

Solar Cell Fabrication: FTO substrates (7 Ω/sq, Pilkington) were etched with zinc powder and HCl (2 M aqueous solution) to give the desired electrode patterning. The substrates were cleaned with Hellmanex (2% by volume in water), de-ionized water, acetone, and ethanol. Oxygen plasma cleaning was then used to remove the last traces of organics. The FTO sheets were subsequently coated with a compact layer of TiO_2 (70 nm) by aerosol spray pyrolysis deposition at 270°C, using titanium diisopropoxide bis(acetylacetonate) in anhydrous ethanol as precursor solution (volume ratio 1:10) and oxygen as carrier gas. The TiO_2 films were heated over 3 hours and allowed to sinter for 30 min in air at 500°C. Once cooled, the samples were immersed into a 15 mM $TiCl_4$ aqueous solution for 45 min at 70°C and then heated again to 500°C for another sintering step of 45 min. 300 nm of mesoporous Al_2O_3 layer was deposited by spin coating (speed 2000 rpm, ramp 2000 rpm/s, time 60 s) a colloidal dispersion of < 50 nm Al_2O_3 nanoparticles at 10 wt% in isopropanol. The samples were then heated at 150°C for 30 min to remove any residual of isopropanol. Upon cooling to room temperature, the perovskite layer was deposited in a nitrogen-filled glovebox by spin coating (speed 2000 rpm, ramp 2000 rpm/s, time 60 s) from 40 wt% DMF solution of methylammonium iodide and $PbCl_2$ (3:1 molar ratio). The substrate was then heated at 100°C for 2 hours on a hotplate in the glovebox. On the top of the perovskite layer an additional 100 nm thick mesoporous Al_2O_3 layer was deposited dropping a colloidal dispersion of < 50 nm Al_2O_3 nanoparticles at 2 wt% in isopropanol on a substrate spinning at 2000 rpm. The samples were then heated at 100°C for 10 min to remove any residual of isopropanol. After cooling at room temperature, iodopentafluorobenzene (IPFB) was deposited as previously reported.[8] The hole transporter material (HTM) was infiltrated within Al_2O_3 overlayer by spin coating (speed 2000 rpm, ramp 2000 rpm/s, time 60s) from chlorobenzene solution. We highlight here that the additives composition commonly use to dope the HTM lithium bis(trifluoromethanesulfonyl)imide (Li-TFSI) and tert-butylpyridine (tBP) was replaced by the protic ionic liquid bis(trifluoromethanesulfonyl)imide (H-TFSI, from Aldrich, CAS Number 82113-65-3) and the inert salt tetraethyl bis-(trifluoromethane)sulfonimide (Et_4N-TFSI, from Aldrich, CAS Number 161401-26-9). The effect of these two chemicals on the charge transport and the device performances has been reported elsewhere.[9] The reason of using the new additive composition is mainly because Li-TFSI need oxygen to effectively dope the HTM, where H-TFSI can work in inert atmosphere, such as the glovebox condition that we made use here. Furthermore, we found that in presence of lithium salts devices are significantly more unstable to air exposure. A complete comparison between the Li-TFSI and the H-TFSI on the device stability is currently under investigation and will be published elsewhere. To prepare the HTM solutions, 40 mM of HTM in chlorobenzene with addition of 3 mol% of H-TFSI (from a stock solution of 0.27 M in acetonitrile) was prepared. This solution was left in a close vial for 3 hours at 100°C to thermally activate the doping mechanism.[9] After cooling down to room temperature, 25 mol% of Et_4N-TFSI (from a stock solution of 0.27 M in chlorobenzene:acetonitrile 9:1 v:v) was added to the solution. We note that the whole preparation was performed in nitrogen-filled glovebox and all the solvent were anhydrous. Finally, back contacts were applied by thermal evaporation of 150 nm of silver.

Device Characterisation. For measuring the performance of the solar cells, simulated sunlight was generated with a class AAB ABET solar simulator calibrated to give simulated AM 1.5, of 100 mW cm^{-2} equivalent irradiance, using an NREL-calibrated KG5 filtered silicon reference cell. The current-voltage curves were recorded with a sourcemeter (Keithley 2400, USA) scanning at 0.15 V/s from 1.4 to 0 V. Scan-rate and scan-direction dependence of the current-voltage curves, which were reported in literature for similar perovskite devices[10], were minimized making use of the IPFB treatment as previously demonstrated.[8]

Supporting Information Figures

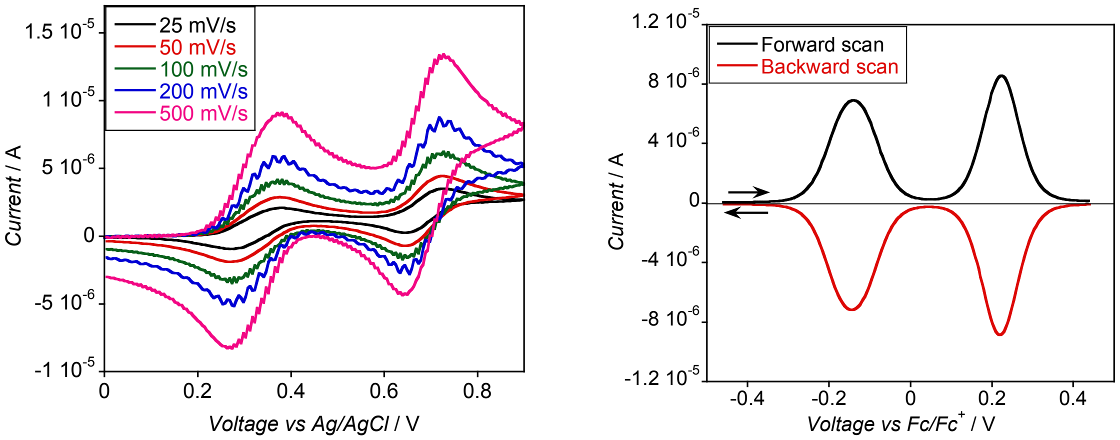

Figure S1. Cyclic (*left*) and square-wave (*right*) voltammetries of **Me$_2$N-DATPA** performed in 0.3 M [TBA][PF$_6$] CH$_2$Cl$_2$ solution and referenced internally to ferrocene (not shown).

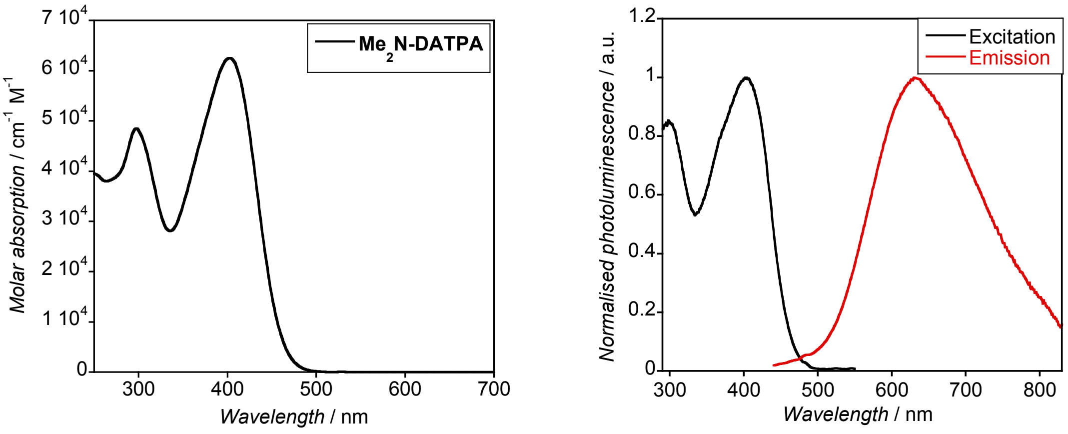

Figure S2. UV-Visible absorption (*left*) and photoluminescence (*right*) spectra of **Me$_2$N-DATPA** acquired in CH$_2$Cl$_2$ solution at $2\cdot10^{-5}$ M and $5\cdot10^{-6}$ M, respectively.

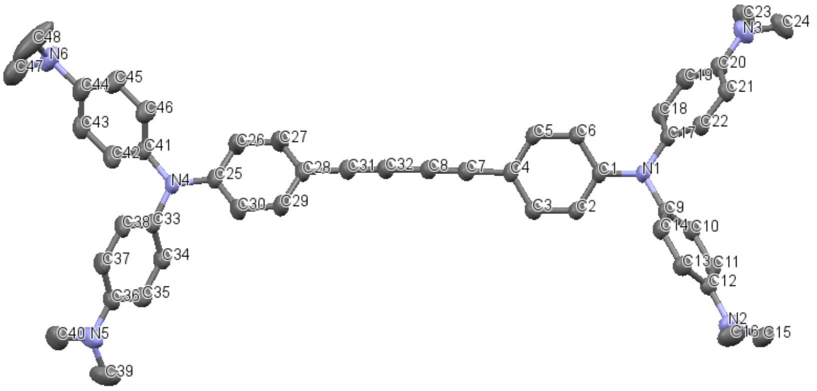

Figure S3. Asymmetric unit of **Me_2N-DATPA** showing atom labels and with probability elipsoids set at 50%

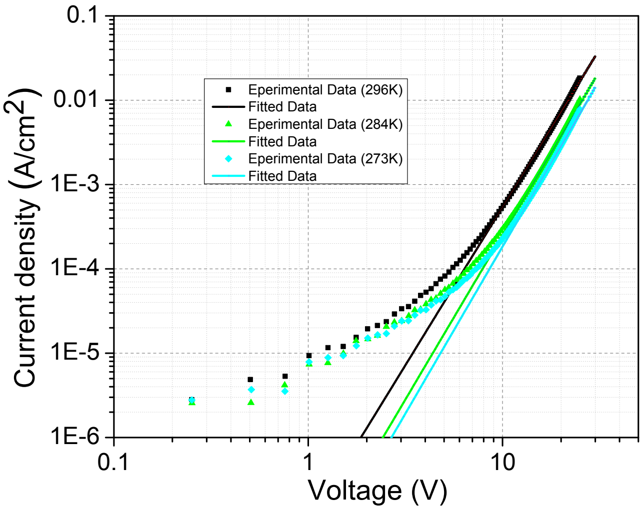

Figure S4. *J–V* data at different temperatures for SCLC method of hole-mobility determination. The resulting mobilities at various temperatures were $\mu/cm^2V^{-1}s^{-1}$ = 1.2 x 10^{-5} (296 K), 8.8 x 10^{-6} (284 K) and 7.6 x 10^{-6} (273 K).

Supporting Information Tables

Table S1. Crystal data and structure refinement for **Me_2N-DATPA**.

Chemical formula (moiety)	$C_{48}H_{48}N_6$	
Chemical formula (total)	$C_{48}H_{48}N_6$	
Formula weight	708.92	
Temperature	120(2) K	
Radiation, wavelength	CuKα, 1.54184 Å	
Crystal system, space group	monoclinic, P 21/n	
Unit cell parameters	a = 9.85327(19) Å	α = 90°
	b = 11.5888(3) Å	β = 95.691(2)°
	c = 34.7326(7) Å	γ = 90°
Cell volume	3946.48(16) $Å^3$	
Z	4	
Calculated density	1.193 g/cm^3	
Absorption coefficient μ	0.546 mm^{-1}	
F(000)	1512	
Crystal colour and size	dark yellow, 0.268 × 0.092 × 0.033 mm^3	
Reflections for cell refinement	7928 (θ range 4.0 to 72.1°)	
Data collection method	Agilent Technologies SuperNova	
	ω scans	
θ range for data collection	4.0 to 76.3°	
Index ranges	h −12 to 12, k −12 to 14, l −43 to 43	
Completeness to θ = 67.7°	100.0 %	
Reflections collected	46934	
Independent reflections	8129 (R_{int} = 0.0613)	
Reflections with $F^2>2\sigma$	5482	
Absorption correction	gaussian	

Min. and max. transmission	0.955 and 0.991
Structure solution	direct methods
Refinement method	Full-matrix least-squares on F^2
Data / restraints / parameters	8129 / 0 / 495
Final R indices [$F^2>2\sigma$]	R1 = 0.0621, wR2 = 0.1514
R indices (all data)	R1 = 0.0976, wR2 = 0.1717
Goodness-of-fit on F^2	1.038
Extinction coefficient	0
Largest and mean shift/su	0.000 and 0.000
Largest diff. peak and hole	0.54 and –0.56 e $Å^{-3}$

References

1. M. Planells, A. Abate, D. J. Hollman, S. D. Stranks, V. Bharti, J. Gaur, D. Mohanty, S. Chand, H. J. Snaith and N. Robertson, *J. Mat. Chem. A*, 2013, **1**, 6949.
2. M. Cossi, N. Rega, G. Scalmani and V. Barone, *J. Comput. Chem.*, 2003, **24**, 669.
3. M. J. Frisch, G. W. Trucks, H. B. Schlegel, G. E. Scuseria, M. A. Robb, J. R. Cheeseman, G. Scalmani, V. Barone, B. Mennucci, G. A. Petersson, H. Nakatsuji, M. Caricato, X. Li, H. P. Hratchian, A. F. Izmaylov, J. Bloino, G. Zheng, J. L. Sonnenberg, M. Hada, M. Ehara, K. Toyota, R. Fukuda, J. Hasegawa, M. Ishida, T. Nakajima, Y. Honda, O. Kitao, H. Nakai, T. Vreven, J. A. Montgomery, J. E. Peralta, F. Ogliaro, M. Bearpark, J. J. Heyd, E. Brothers, K. N. Kudin, V. N. Staroverov, R. Kobayashi, J. Normand, K. Raghavachari, A. Rendell, J. C. Burant, S. S. Iyengar, J. Tomasi, M. Cossi, N. Rega, J. M. Millam, M. Klene, J. E. Knox, J. B. Cross, V. Bakken, C. Adamo, J. Jaramillo, R. Gomperts, R. E. Stratmann, O. Yazyev, A. J. Austin, R. Cammi, C. Pomelli, J. W. Ochterski, R. L. Martin, K. Morokuma, V. G. Zakrzewski, G. A. Voth, P. Salvador, J. J. Dannenberg, S. Dapprich, A. D. Daniels, Farkas, J. B. Foresman, J. V. Ortiz, J. Cioslowski and D. J. Fox, *Gaussian 09, Revision B.01*, Gaussian Inc, Wallingford CT, 2009.
4. M. Hanwell, D. Curtis, D. Lonie, T. Vandermeersch, E. Zurek and G. Hutchison, *J. Cheminf.*, 2012, **4**, 17.
5. Agilent Technologies, 2011, CrysAlisPro, Agilent Technologies UK Ltd, Oxford, UK.
6. A. Altomare, G. Cascarano, C. Giacovazzo, A. Guagliardi, M. C. Burla, G. Polidori and M. Camalli, *J. Appl. Crystallogr.*, 1994, **27**, 435.
7. G. Sheldrick, *Acta Crystal.*, 2008, **64**, 112.
8. *Nano Lett.*, **2014**, *14* (6), pp 3247–3254
9. *J. Am. Chem. Soc.*, **2013**, *135* (36), pp 13538–13548
10. *J. Phys. Chem. Lett.*, **2014**, *5* (9), pp 1511–1515